Spectral and Magnetic Properties of α- and γ-Ce from Dynamical Mean-Field Theory and Local Density Approximation

M. B. Zölfl,[1] I. A. Nekrasov,[2] Th. Pruschke,[1] V. I. Anisimov,[2] and J. Keller[1]

[1]*Institut für Theoretische Physik I, Universität Regensburg, Universitätsstrasse 31, 93053 Regensburg, Germany*

[2]*Institute for Metal Physics, 620219 Yekaterinburg GSP-170, Russia*

(Received 18 January 2001; published 13 December 2001)

We present excitation spectra for Ce metal obtained with an *ab initio* scheme combining local density approximation and dynamical mean-field theory including itinerant spd and correlated f states. The local interactions among the f electrons lead to typical many-body resonances in the f density of states (DOS), such as lower and upper Hubbard bands and the Kondo resonance. The spd DOS show weak renormalization effects due to hybridization. We observe different Kondo temperatures for α- and γ-Ce due to strong volume dependence of the effective hybridization strength for the localized f electrons. Finally we compare our results with a variety of experimental data.

DOI: 10.1103/PhysRevLett.87.276403 PACS numbers: 71.27.+a, 74.25.Jb

Ce metal is the simplest lanthanide compound with only one atom in a face centered cubic (fcc) crystal structure and a relatively small set of relevant electronic states derived from s, p, d, and f orbitals of Ce. It shows a unique isostructural (fcc to fcc) $\alpha \rightarrow \gamma$ phase transition with increasing temperature. The high-temperature γ phase has 15% larger volume and displays a Curie-Weiss-like temperature dependence of the magnetic susceptibility signaling the existence of local magnetic moments while the α phase shows a Pauli-like temperature independent paramagnetism [1].

While many different models were proposed to describe this system (for a review see [2]), the most relevant seems to be the periodic Anderson model (PAM). Studies based on the single impurity Anderson model [3], which with some caution can be viewed as a zeroth-order approximation to the PAM, with a hybridization function obtained from local density approximation (LDA) band structure calculations were rather successful in reproducing Kondo scales and spectra for α- and γ-Ce. However, empirical renormalizations of the hybridization function and position of the impurity level were needed for satisfactory agreement between calculated and experimental spectra. In addition, Laegsgaard *et al.* [4] states that a rescaling of the hybridization function is necessary in order to describe the phase transition. Recently, quantum Monte Carlo calculations for the PAM with a phenomenological form of the hybridization have been performed [5]. Since the physics of the system critically depends on the behavior of this quantity in the vicinity of the Fermi level [6], results obtained within simplified models can serve only to elucidate qualitative aspects. In addition, the temperature accessible in these calculations is too high to make reliable statements about possible low-energy scales in the case of γ-Ce.

Because of the development of the dynamical mean-field theory (DMFT) [7] and the recently proposed combination of DFT/LDA and DMFT [8–17] a more realistic treatment of Ce systems is now possible, as has been demonstrated recently for the Ce monopnictides [18]. Here we present results obtained within LDA + DMFT(NCA) [11,19] for Ce metal.

In contrast to the Hubbard model (degenerate and nondegenerate), where hybridization occurs only between correlated d or f orbitals, Ce is much more complicated. The direct f-f hybridization is of the same order of magnitude as the hybridization of f orbitals with the delocalized spd states. Thus in order to describe Ce we even have to go beyond the standard periodic Anderson model and use the full (s, p, d, f) basis set for the Hamiltonian.

In the following we will concentrate on a simplified local interaction. Thus we introduce only two distinct Coulomb parameters: the intraorbital Coulomb energy U in case of a doubly occupied orbital and the interorbital Coulomb energy U' for a doubly occupied f shell with electrons on f orbitals with different indices. Since we neglect any exchange correlations, which are typically of the order of one tenth of the Coulomb interaction, $U = U'$ in order to fulfill the condition of rotational invariance of the local interaction [20]. The inclusion of the full local Coulomb interaction has already been investigated [11] and is in principle possible here, too. However, because of the large number of f orbitals the inclusion of the full Coulomb matrix is currently too cumbersome from a computational point of view. We thus arrive at an interaction of the form

$$H_{\mathrm{corr}}^{\mathrm{local}} = U \sum_{m} \hat{n}_{m\uparrow}\hat{n}_{m\downarrow} + \frac{U'}{2} \sum_{m,m',\sigma,\sigma'}^{m\neq m'} \hat{n}_{m\sigma}\hat{n}_{m'\sigma'}. \quad (1)$$

The most important feature of the DMFT is that the proper one-particle self-energy due to the local Coulomb interaction is purely local [7]. Thus, we obtain as an expression for the full Green function of the interacting system

$$\mathsf{G}(z) = \frac{1}{N} \sum_{\vec{k}} [z\mathsf{I} - \mathsf{h}(\vec{k}) - \Sigma(z)\mathsf{I}_f]^{-1}, \quad (2)$$

where the noninteracting one-particle Hamiltonian $\mathsf{h}(\vec{k})$ and consequently $\mathsf{G}(z)$ will in general be matrices in

orbital space; I_f is the diagonal matrix with matrix elements equal 1 for f orbitals and zero for all others, and I is the unit matrix. The $\vec{k}$ summation is done by a standard tetrahedron method [8]. Within this method one can easily treat hybridization effects between correlated and noncorrelated states.

As starting point of our calculation we determined the one particle LDA Hamiltonian with the LMTO method [21] considering the $6s$, $6p$, $5d$, and $4f$ shells. The noninteracting one-particle Hamiltonian $\mathsf{h}(\vec{k})$ was obtained by subtracting the Hartree contribution of (1) from the LDA results in order to avoid double counting [8,11,12]. The value of the Coulomb interaction was calculated by a supercell method [22] and found to be $U \approx 6$ eV. The chemical potential was adjusted to conserve the number of particles (4 electrons per site) during the self-consistent LDA + DMFT calculation. Analyzing the partial densities of states one can observe for both α- and γ-Ce at a temperature of $T = 580$ K renormalization effects, in particular, broadening and shifts of structures, for s and d states but only marginal effects for the p states. This is a consequence of the hybridization, which is seen by a nonvanishing s or d density at the position of the f states in the LDA result. The f states are strongly renormalized. A lower Hubbard band (LHB) is observed at the position of the corrected (double counting) LDA f state at about -3 eV. The upper Hubbard band (UHB) is situated at about 4.5 eV and describes an excitation of a doubly occupied f state. At the Fermi level one observes a Kondo resonance (KR) for α-Ce, which can be described by a singlet formation between an unpaired f electron and the surrounding conduction electrons. The d-density for α-Ce shows an onset of a hybridization gap, which is well known in model calculations for the periodic Anderson model [23] and is a consequence of the formation of the singlet state between the unpaired f spins and the conduction electrons. For γ-Ce one observes only the onset of a KR as a consequence of the smaller T_K compared to the α phase, and thus no hybridization gap opens in the conduction electron density.

In Table I we show a comparison of our results with the results of spectral fits to electron [3] and high-energy neutron spectroscopy [24]. In [3] the spectral fits were done by using a hybridization function obtained from a standard LDA calculation, which served as a basis to calculate the spectral functions of a single impurity Anderson model. However, it turned out that LDA cannot reproduce the experimental data satisfactorily. Thus a compensating factor κ multiplied to the hybridization function explained by a self-interaction correction argument was introduced. In contrast to this work, we use a parameter-free *ab initio* calculation to explain the experimental results. The occupation probabilities are in fair agreement with [3], as well as the number of f electrons per site, n_f. The occupation probabilities P_0, P_1, and P_2 for the states f^0, f^1, and f^2 were calculated from the particular ionic propagators. The Kondo temperature for α-Ce, $T_{K,\alpha} \approx 1000$ K, is roughly given by the width of the KR. Since for γ-Ce the Abrikosov-Suhl resonance is not yet well developed, it makes no sense to estimate T_K from its width. Instead, for γ-Ce we estimate T_K from the ratio of the hybridization strength at the Fermi level of both considered materials $[\mathrm{Im}\{\Delta_\alpha(\varepsilon_F)\}/\mathrm{Im}\{\Delta_\gamma(\varepsilon_F)\} = 2]$, assuming the standard exponential dependence of T_K on model parameters. With this relation we obtain $T_{K,\gamma} \approx \frac{1}{30} T_{K,\alpha}$ [25]. Since the NCA for multiband models typically underestimates T_K, it is obvious that our absolute values cannot be expected to match with the experiments. The surprisingly good agreement for α-Ce seen in Table I is probably by chance and due to the neglect of Hund's rule coupling and spin-orbit splitting, which typically will lead to a smaller T_K. Nevertheless, the ratio of the Kondo temperatures for the two different phases should be meaningful and is in good agreement with experiment (see Table I). The static susceptibilities $\chi(0)$ calculated with T_K as an input via $\chi(0) = C\frac{1-P_0}{T_K}$ naturally have the same qualitative character. In this formula C is the Curie constant for the lowest $4f$ state with $j = \frac{5}{2}$ and P_0 is the probability of the f^0 state. Again, the ratio of the susceptibilities for both phases are in good agreement with experiment (see Table I). Also included in Table I is the quantity Δ_{av}, which represents the averaged value of the imaginary part of the hybridization function $\mathrm{Im}\{\Delta(\omega)\}$ over an energy interval from -3 to 0 eV [26].

The imaginary part of the hybridization functions in Fig. 1 (full curves) shows strong renormalizations

TABLE I. Comparison between LDA + DMFT(NCA) calculated parameters for both α and γ phases at $T = 580$ K and experimental values.

	α-Ce			γ-Ce		
	LDA + DMFT(NCA)	α-Ce [3]	α-Ce [24]	LDA + DMFT(NCA)	γ-Ce [3]	γ-Ce [24]
P_0	0.126	0.1558		0.0150	0.0426	
P_1	0.829	0.8079		0.9426	0.9444	
P_2	0.044	0.0264		0.0423	0.0131	
n_f	0.908	0.861	0.8	1.014	0.971	1
T_K, (K)	1000	945	1800, 2000	30	95	60
$\chi(0)$, (10^{-3} emu/mol)	1.08	0.70	0.53	24	8.0	12
Δ_{av}, (meV)	86.6	66.3		42.7	32.2	

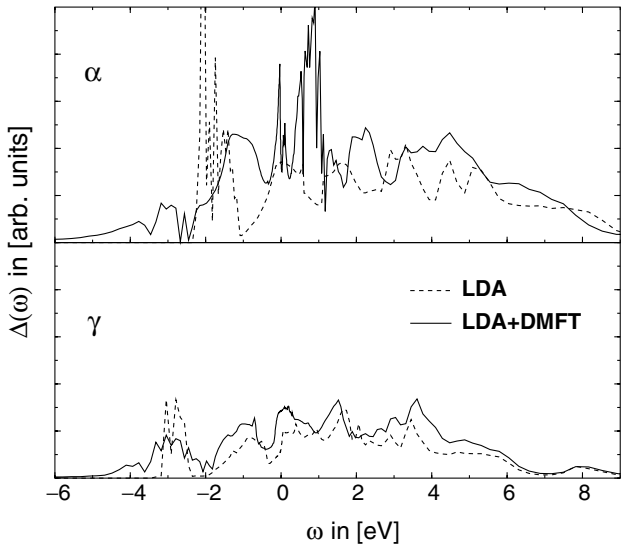

FIG. 1. Imaginary part of the hybridization function in the DMFT (full lines) as compared to the double-counting corrected LDA results (dashed lines).

compared to the double-counting corrected LDA results (dashed curves), especially close to the Fermi energy. This also implies drastic changes of this quantity compared to the one used in Ref. [3]. Note also that the total weight of this quantity for α-Ce is twice as high as the one for the γ phase. Very important is here the inclusion of all s-, p-, and d-conduction states. The use of correlated f states only would produce a too small hybridization at the Fermi energy and thus a too small T_K.

In the PES data for α-Ce in the upper part of Fig. 2 the observed peaks are identified as f contributions to the density of states by a cross section argument using different photon energies [27]. Thus we compare the experiment with the calculated partial density for f states. The theoretical f spectrum shows a LHB which is also seen in the experiment. In contrast to experiment, the calculated LHB appears to be much broader and its center is shifted to lower energies by about 0.5 eV. While the broadening must be attributed to the NCA, the shift can have multiple reasons. For example, an uncertainty in the Coulomb parameter U or the use of the simplified Coulomb interaction (1) may easily account for the discrepancy.

The BIS spectrum for α-Ce shows a main structure between 3 and 7 eV, which is attributed to $4f^2$ final state multiplets. In the calculated spectrum all excitations to $4f^2$ states are described by the featureless UHB. As a consequence of the simplified interaction model all doubly occupied states are degenerate. This shortcoming in our calculation is responsible for the sharp peaked structure of this feature. The neglected exchange interaction would produce a multiplet structure, which would be closer to the experiment. The experimental peak at about 0.5 eV is attributed to two $4f^1$ final states, which are split by spin-orbit coupling. The calculated f spectrum shows a sharp

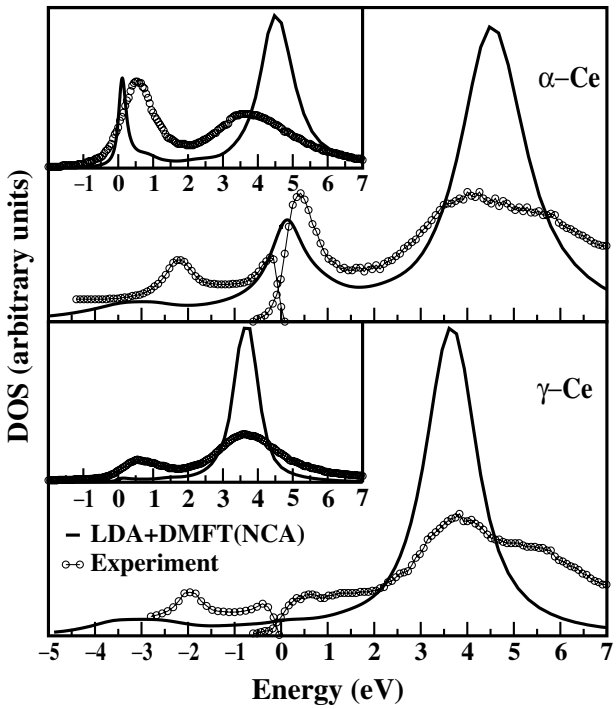

FIG. 2. Comparison between combined PES [27] and BIS [29] experimental (circles) and theoretical (solid line) f spectra for α-Ce (upper part) and γ-Ce (lower part) at $T = 580$ K. The relative intensities of the BIS and PES portions are roughly for one $4f$ electron. The experimental and theoretical spectra were normalized and the theoretical curve was broadened with resolution width of 0.4 eV. In the insets a comparison between RIPES [30] experimental (circles) and theoretical (solid line) f spectra is given. The experimental and theoretical data were normalized and the theoretical curve was broadened with broadening coefficient of 0.1 eV.

KR slightly above the Fermi energy, which is the result of the formation of a singlet state between f and conduction states. We thus suggest that the spectral weight seen in the experiment is a result of this KR. Since we did not yet include spin-orbit coupling in our model, we, of course, cannot observe the mentioned splitting of the resonance. However, as it is well known [28], the introduction of such a splitting would eventually split the KR. If we used the experimentally determined value of about 0.3 eV for the spin-orbit splitting [29], the observed resonance of width 0.5 eV would indeed occur in the calculations.

In the lower part of Fig. 2 a comparison between experiment and our calculation for γ-Ce is shown. The most striking difference between lower and upper figures is the absence of the KR in the high temperature phase (γ-Ce; transition temperature 141 K [1]) which is in agreement with our calculations.

In the insets of Fig. 2 our results for the nonoccupied states in the f density are compared with RIPES data [30]. The calculated f spectra were multiplied by the Fermi-step function and broadened with a Lorentzian of the width 0.1 eV in order to mimic the experimental resolution in

the theoretical curves. Here, as above the theoretical overestimation of the UHB, is a consequence of the simplified local interaction and thus of the missing multiplet structure of the $4f^2$-final states. The main feature of the experimental spectra: strong decreasing of the intensity ratio for KR and UHB peaks going from α to γ phase, can also be seen in the theoretical curves.

In conclusion, we have presented a realization of a combination of density-functional theory in the local density approximation and the dynamical mean-field theory to obtain a first-principles computational scheme for heavy-fermion systems. The scheme was set up for the first time with a combination of correlated and noncorrelated states in order to introduce the important effect of hybridization between s, p, and d states and strongly correlated f states. The solution of the DMFT equations was done by using the noncrossing approximation. We calculated the one-particle spectra for α- and γ-Ce and found Kondo temperature values ($T_{K,\alpha} \approx 1000$ K and $T_{K,\gamma} \approx 30$ K), which explain the experimental results.

We observe quite reasonable results concerning occupation probabilities P_0, P_1, P_2, and the number of f electrons per site n_f. The ratio of T_K and thus the static susceptibilities $\chi(0)$ values for two phases are in fair agreement with the experimental results considering the problems of the NCA method. Moreover, we found qualitative good agreement with PES, BIS, and RIPES experiments, i.e., the positions of LHB, UHB, and the Kondo resonance.

This work was partially supported by the DFG Grant No. PR 298/5-1&2, Russian Foundation for Basic Research Grant No. RFFI-01-02-17063, and the Netherland Organization for the Advance of Pure Science Grant No. NWO 047-008-012.

[1] K. A. Gschneidner, Jr., R. O. Elliott, and R. R. McDonald, J. Phys. Chem. Solids **23**, 1191 (1962); D. C. Koskimaki and K. A. Gschneidner, Jr., Phys. Rev. B **11**, 4463 (1975); J. M. Lawrence and R. D. Parks, J. Phys. (Paris), Colloq. **37**, C4-249 (1976).
[2] A. K. McMahan, C. Huscroft, R. T. Scalettar, and E. L. Pollock, J. Comput.-Aided Mater. Des. **5**, 131 (1998).
[3] L. Z. Liu, J. W. Allen, O. Gunnarsson, N. E. Christensen, and O. K. Andersen, Phys. Rev. B **45**, 8934 (1992).
[4] J. Laegsgaard and A. Svane, Phys. Rev. B **59**, 3450 (1999).
[5] K. Held, C. Huscroft, R. T. Scalettar, and A. K. McMahan, Phys. Rev. Lett. **85**, 373 (2000).
[6] P. J. G. van Dongen, K. Mujamdar, C. Hushcroft, and F. C. Zhang, cond-mat/0011119.
[7] D. Vollhardt, in *Correlated Electron Systems,* edited by V. J. Emery (World Scientific, Singapore, 1993), p. 57; Th. Pruschke, M. Jarrell, and J. K. Freericks, Adv. Phys. **44**, 187 (1995); A. Georges, G. Kotliar, W. Krauth, and M. J. Rozenberg, Rev. Mod. Phys. **68**, 13 (1996).
[8] V. I. Anisimov, A. I. Poteryaev, M. A. Korotin, A. O. Anokhin, and G. Kotliar, J. Phys. Condens. Matter **9**, 7359 (1997).
[9] H. Kajueter and G. Kotliar, Int. J. Mod. Phys. **11**, 729 (1997).
[10] A. I. Lichtenstein and M. I. Katsnelson, Phys. Rev. B **57**, 6884 (1998).
[11] M. B. Zölfl, Th. Pruschke, J. Keller, A. I. Poteryaev, I. A. Nekrasov, and V. I. Anisimov, Phys. Rev. B **61**, 12 810 (2000).
[12] I. A. Nekrasov, K. Held, N. Blümer, A. I. Poteryaev, V. I. Anisimov, and D. Vollhardt, Eur. Phys. J. B **18**, 55 (2000).
[13] K. Held, I. A. Nekrasov, N. Blümer, V. I. Anisimov, and D. Vollhardt, e-print cond-mat/0010395.
[14] M. J. Rozenberg, Phys. Rev. B **55**, R4855 (1997); J. E. Han, M. Jarrell, and D. L. Cox, Phys. Rev. B **58**, R4199 (1998); K. Held and D. Vollhardt, Eur. Phys. J. B **5**, 473 (1998).
[15] M. I. Katsnelson and A. I. Lichtenstein, J. Phys. Condens. Matter **11**, 1037 (1999).
[16] M. I. Katsnelson and A. I. Lichtenstein, e-print cond-mat/9904428.
[17] A. Liebsch and A. Lichtenstein, Phys. Rev. Lett. **84**, 1591 (2000).
[18] J. Laegsgaard and A. Svane, Phys. Rev. B **58**, 12 817 (1998).
[19] H. Keiter and J. C. Kimbal, Phys. Rev. Lett. **25**, 672 (1970); N. E. Bickers, D. L. Cox, and J. W. Wilkins, Phys. Rev. B **36**, 2036 (1987).
[20] K. Held and D. Vollhard, Eur. Phys. J. B **5**, 473 (1998).
[21] O. K. Andersen, Phys. Rev. B **12**, 3060 (1975).
[22] V. I. Anisimov and O. Gunnarsson, Phys. Rev. B **43**, 7570 (1991).
[23] Th. Pruschke, R. Bulla, and M. Jarrell, Phys. Rev. B **61**, 12 799 (2000).
[24] A. P. Murani, Z. A. Bowden, A. D. Taylor, R. Osborn, and W. G. Marshall, Phys. Rev. B **48**, 13 981 (1993).
[25] E. Müller-Hartmann, Z. Phys. B **57**, 281 (1984).
[26] In our approach we use no compensation factor κ, which was used in [3] in order to consider the effect of a self-interaction correction.
[27] D. M. Wieliczka, C. G. Olson, and D. W. Lynch, Phys. Rev. B **29**, 3028 (1984).
[28] T. A. Costi, Phys. Rev. Lett. **85**, 1504 (2000).
[29] E. Wuilloud, H. R. Moser, W. D. Schneider, and Y. Baer, Phys. Rev. B **28**, 7354 (1983).
[30] M. Grioni, P. Weibel, D. Malterre, Y. Baer, and L. Duo, Phys. Rev. B **55**, 2056 (1997).